Enhancement of the Signal-to-Noise Ratio in $H_2{}^{15}O$ Bolus PET Activation Images: A Combined Cold-Bolus, Switched Protocol

Jorge J. Moreno-Cantú, Christopher J. Thompson, Ernst Meyer, Pierre Fiset, Robert J. Zatorre, Denise Klein, and David C. Reutens

Department of Neurology and Neurosurgery, Neuropsychology/Cognitive Neuroscience Unit, and McConnell Brain Imaging Center, Montreal Neurological Institute, Montreal, Quebec; and Department of Anaesthesiology, Royal Victoria Hospital, McGill University, Montreal, Quebec, Canada

To increase the signal-to-noise ratio (S/N) of $H_2{}^{15}O$ bolus PET activation images, we designed and tested a data acquisition protocol that alters the relative distribution of tracer in the uptake and washout phases of the input function. This protocol enhances the S/N gains obtained with conventional switched protocols by combining task switching and the use of a large bolus of blood free of tracer (cold bolus). The cold bolus is formed by sequestering blood in the lower limbs with a double cuff before tracer injection. **Methods:** The effect of a combined cold-bolus, switched protocol on the signal from activation images was first simulated using a compartmental model of the uptake of $H_2{}^{15}O$ into the brain. Then, the effectiveness of the protocol was investigated in 4 healthy volunteers performing a language task. Each volunteer underwent scanning 12 times: 3 activation/baseline and 3 baseline/activation scans using the conventional switched protocol and 3 activation/baseline and 3 baseline/activation scans using the combined cold-bolus, switched protocol. The S/N changes introduced when using the cold bolus were analyzed by comparing, across protocols, the magnitude and statistical significance of the activation foci associated with the execution of the language task identified in the averaged subtracted images, and by comparing image noise levels. **Results:** In the simulated datasets, the combined protocol yielded a substantial increase in the activation signals for scan durations greater than 60 s, in comparison with equivalent signals yielded by the switched protocol alone. In the PET experiments, activation foci obtained using the combined protocol had significantly higher *t* statistic values than did equivalent foci detected using the conventional switched protocol (mean improvement, 36%). Analysis of the S/N in the averaged subtracted images revealed that the improvements in statistical significance of the activation foci were caused by increases in the signal magnitudes and not by decreases in overall image noise. **Conclusion:** We designed a data acquisition protocol for $H_2{}^{15}O$ bolus PET activation studies that combines the use of a tracer-free bolus with a switched protocol. Simulated and experimental data suggest that this combined protocol enhances the S/N gains obtained with a conventional switched protocol. Implementation of the combined protocol in $H_2{}^{15}O$ bolus activation studies was easy.

Received Jun. 15, 1999; revision accepted Aug. 4, 1999.

For correspondence or reprints contact: Jorge J. Moreno-Cantú, PhD, PET Imaging Service (11P), VA Medical Center, 1 Veterans Dr., Minneapolis, MN 55417.

Key Words: PET; switched protocol; activation studies; water; signal-to-noise ratio

J Nucl Med 2000; 41:926–933

Studies of brain function using PET and $H_2{}^{15}O$ as a freely diffusible tracer depend on the relationship between uptake of tracer by the brain and regional cerebral blood flow (rCBF) (*1–3*). In these studies, brain activity is often identified by comparing images from different mental states (e.g., activation versus baseline) or by parametrically modifying task variables across activation images collected minutes apart (*4–7*). Typically, PET images are acquired while a subject continuously performs a task (standard activation protocol). Because the linear correlation between the detected counts and rCBF is confined to the first 40–60 s after a bolus injection of $H_2{}^{15}O$, data acquisition protocols designed to quantitatively assess rCBF differences between mental states using $H_2{}^{15}O$ are constrained to that time span (*1,2*). Unfortunately, with such short imaging periods, a significant portion of the image-forming photons available after bolus injection is wasted. If the quantitative estimation of rCBF is not required, activity-concentration images obtained using standard activation protocols and scans 60–100 s long can be used. These scanning times yield datasets with larger signal-to-noise ratios (S/N) than those obtained with protocols estimating rCBF quantitatively (*8–10*). However, scans longer than 100–120 s are not typically used because the signal difference between activated and baseline states is maintained for only about 2 min after the tracer is detected in the brain. Prolonging the acquisition of data beyond those times when using standard activation protocols generally decreases the S/N of PET images (*10–11*). This effect can be explained as follows. When the tracer concentration in arterial blood is high (seconds after bolus injection), the difference in blood flow between activated and baseline states yields a relative accumulation of tracer in the activated brain region (uptake phase). As the arterial concentration of tracer decreases, the

difference in tissue radioactivity between activation and baseline states decreases. This decrease is caused by the higher unidirectional transfer of tracer from brain to blood (washout phase) that is introduced by maintaining the difference in blood flow when the arterial concentration of tracer is low. During the washout phase, increasing the scan length decreases the relative difference between signals from activated and baseline regions. Thus, although the image noise is reduced as the acquisition length is increased, the difference between activation and baseline signals decreases at a faster rate, resulting in a decrease in the S/N of subtracted activation images (*10–12*). Nevertheless, the S/N can be increased by manipulating tracer distribution to maximize scan length using a switched protocol (*11,12*). This result is achieved by switching task execution from activation to baseline during the activation scans and vice versa during the baseline scans when tracer concentration in the brain peaks (typically 50–80 s after bolus injection) (*11*). The effect of task switching is 2-fold: first, after task execution is switched from activation to baseline, blood flow in the regions activated by the activation task is decreased, thereby reducing tracer clearance, whereas blood flow in regions activated by the baseline task is increased, thereby augmenting tracer clearance; second, after task execution is switched from baseline to activation, the opposite occurs. When using a switched protocol, the difference in tissue radioactivity in activated and baseline states can be maintained for approximately 4 min (*11*).

Here, we describe a method to augment the S/N of subtracted activation images obtained with the switched protocol by decreasing tracer dispersion during the uptake stage and by enhancing tracer clearance during the washout period. This goal is accomplished by combining task switching with a reduction in the blood pool available for tracer mixing during the uptake period and with the release of a large cold bolus during the washout period. The blood-pool reduction is achieved by occluding blood circulation to the lower limbs before tracer injection; the cold-bolus effect is achieved by releasing the blood previously sequestered in the legs. In a healthy adult, the lower limbs contain 10%–40% of the total blood volume, depending primarily on body position and limb temperature (*13–15*). The effect of combining a cold bolus and a switched protocol on the activation signals was first simulated using a compartmental model of $H_2{}^{15}O$ uptake in the brain (*1,16*). The combined protocol was then tested in a PET activation experiment designed to identify the neuronal substrates activated when subjects generate elements from a given category (e.g., the subject is given the category "mineral" and generates an element from it such as "zinc"). This experiment monitors lexical-search and retrieval operations that have been extensively studied using PET in our laboratories (*12,17,18*).

MATERIALS AND METHODS

Simulation Studies

The kinetics of uptake of $H_2{}^{15}O$ into brain tissue were simulated using a 1-compartment model (*1,16*). In this model, for a constant cerebral blood flow (F), the radioactivity (M) in the brain at a time $t = T$ after tracer injection is described by:

$$M(T) = F\int_0^T C_a(t)e^{(F/P+\lambda)(t-T)}\,dt, \qquad \text{Eq. 1}$$

where C_a is the concentration of tracer in arterial blood, λ is the decay constant for ^{15}O, and P is the partition coefficient across the blood–brain barrier and is assumed to have a value of 0.9 mL/g. Thus, if the rCBF (F_2) changes at time T_s, the radioactivity in the brain at any time T_2 after T_s is given by:

$$M(T_2) = M(T_S)e^{(F_2/P+\lambda)(T_s-T_2)} + F_2\int_{T_S}^{T_2} C_a(t)e^{(F_2/P+\lambda)(t-T_2)}\,dt. \qquad \text{Eq. 2}$$

Input Functions. A typical measured input function (*19*) was used to simulate tracer kinetics in standard and switched protocols (Fig. 1). This input function was then modified to account for the blood volume and tracer concentration changes introduced by the cold-bolus, switched protocol. First, we simulated the reduction in the whole-body vascular volume available for tracer dispersion caused by the isolation of the vasculature of the lower limbs. A scaling factor of 1.2 was applied to the first 60 s of the typical input function to simulate a 25% decrease in the blood volume available for dispersion (*13–15*). Second, we simulated incomplete mixing of the tracer-free blood released after cuff deflation. Here, the input function was multiplied elementwise by a time-varying scaling factor (R_2) of the form:

$$R_2(t) = 1 \qquad t < T_S$$

$$= 1 - \frac{R}{A[\max(R) - \min(R)]} \qquad t \geq T_S, \qquad \text{Eq. 3}$$

where t is the time after injection, T_s is the time when the cuffs were deflated (60 s), and R is of the form:

$$R(t) = \left[\frac{\alpha(t - T_S)}{\delta^2}e^{[-(t-T_S)/\delta+\beta]}\right]e^{-\lambda(t-T_S)}. \qquad \text{Eq. 4}$$

In the simulation, we used $\alpha = 625$, $\beta = 1$, $\delta = 20$, $\lambda = 0.1$, and $A = 2$. Equations 3 and 4 generate a pattern comparable with that created by a fast bolus injection, only inverted (i.e., a sudden tracer-concentration decrease followed by an asymptotic return to prebolus tracer-concentration values). The magnitudes for the 5 parameters were empirically selected to create a realistic inverted bolus.

Time–Activity Curves. The values for blood flow used in all simulations were 50 mL/100 g/min for mean whole-brain blood flow; 65 mL/100 g/min for flow in gray matter in the baseline state, and 91 mL/100 g/min for flow in activated gray matter. Baseline and activation flow values were chosen to match those used by Cherry et al. (*11*) for their evaluation of switched protocols to facilitate across-study comparisons. Estimations of normal baseline flow values have been reported by Perlmutter et al. (*20*) and Frackowiak et al. (*21*). Simulations of tracer concentration in gray matter in 3-min scans using standard; switched; and combined cold-bolus, switched protocols were performed. Activity concentration curves for a gray matter region were then integrated over the simulated scan lengths and normalized by whole-brain radioactivity. Whole-brain radioactivity was simulated using Equation 1 for

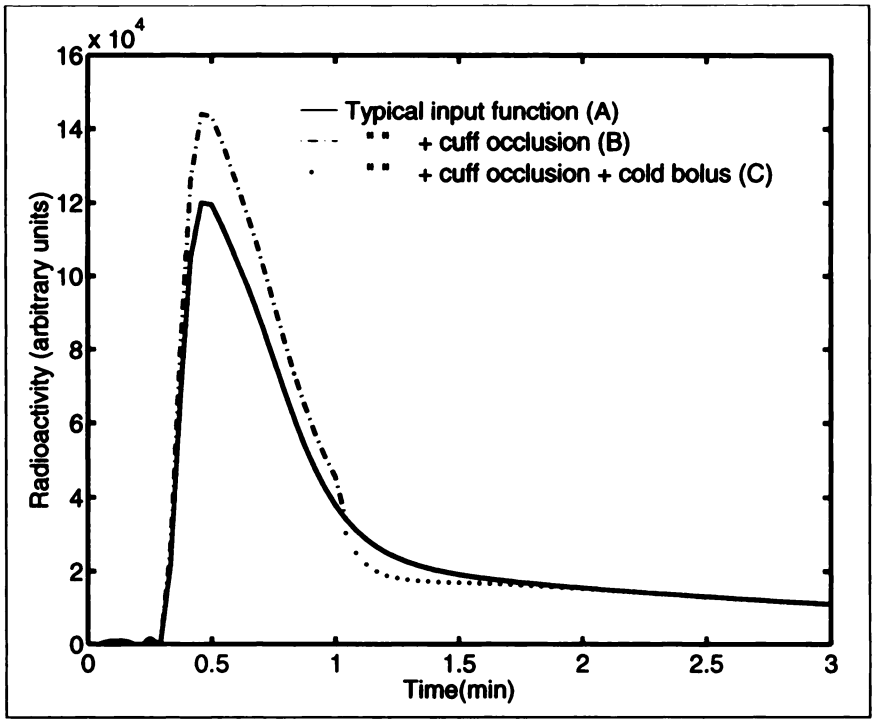

FIGURE 1. Input functions used to simulate tracer uptake in standard, switched, and combined cold-bolus, switched protocols. (A) Standard- and switched-protocol simulations used typical measured input function (*19*). (B and C) Cold-bolus, switched-protocol simulations used 2 input functions obtained by modifying measured function. Function B accounted for 60-s cuff occlusion and instantaneous mixing of cold bolus. Function C accounted for 60-s cuff occlusion plus realistic time-varying mixing of cold bolus after cuff deflation.

each input function, assuming that whole-brain blood flow did not change. The normalizing factor was the integral of whole-brain radioactivity over the duration of simulated scan lengths. The resulting time–activity curves are shown in Figure 2. Tracer concentration for a standard activation protocol was simulated using the measured input function and activated and baseline blood flows that were kept constant for the duration of the scans. The switched protocol was simulated using the measured input function and blood flows corresponding to switching task execution at 60 s. Tracer uptake in the cold-bolus, switched protocol was simulated using 2 different input functions for blood flows, corresponding to switching tasks and deflating the cuffs at 60 s. Both input functions accounted for the initial decrease in the available blood volume. However, 1 input function simulated instantaneous complete mixing of the cold bolus after cuff deflation, whereas the other simulated time-dependent incomplete mixing. For the switched and the combined cold-bolus, switched protocols, the baseline/activation scans consisted of a baseline condition followed by the

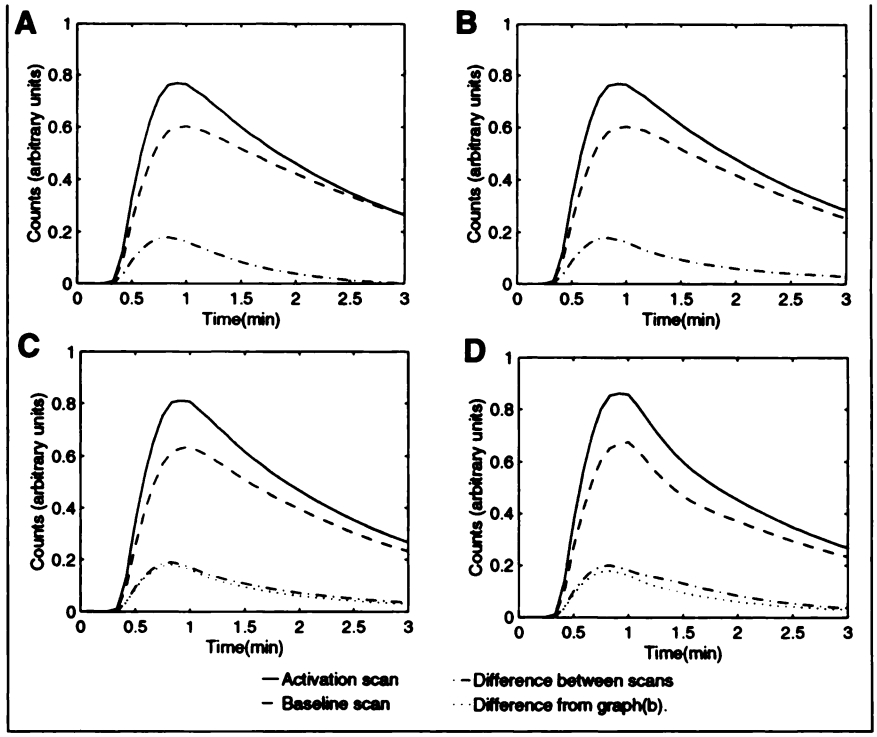

FIGURE 2. Simulated tracer concentration in activated and baseline gray matter in scans using standard protocol (A), switched protocol (B), switched protocol with 60-s cuff occlusion and instantaneous mixing of cold bolus (C), and switched protocol with 60-s cuff occlusion and realistic time-varying mixing of cold bolus (D). Bottom plots in A and B represent difference in activity concentration between activation and baseline states. C and D show equivalent plots and, as reference, bottom plot from B.

activation condition. In the activation–baseline scans, the order of task conditions was reversed.

Signal Magnitude Versus Statistical Variability. To examine the relative value (V) of the activation signal in a subtracted image with respect to its estimated statistical uncertainty, we used:

$$V = \frac{A - B}{\sqrt{A + B}}, \qquad \text{Eq. 5}$$

where A and B are the counts in the activation and baseline study. Figure 3 shows V for the simulated protocols against scan duration.

PET Experiments

The effect of using a combined cold-bolus, switched protocol on the S/N of activation images was investigated using 48 3-dimensional PET scans collected from 4 healthy volunteers. All were male, right handed, and native English speakers (mean age, 24 y). Informed consent was obtained from all volunteers, and the protocol was approved by the Ethics Committee of the Montreal Neurological Institute and Hospital. PET brain scans were acquired using a ECAT HR+ (CTI Inc., Knoxville, TN) whole-body 3-dimensional scanner, a 32-ring tomograph with an axial field of view of 15.5 cm, and 18,432 bismuth-germanate crystals (*22*). The scanner has transaxial resolutions of less than 5.1 mm and 6.6 mm, full-width at half-maximum, at 1 cm and 10 cm, respectively, from the center of the field of view.

Cognitive Tasks. The neuronal regions activated when generating an element from a given category were studied using an activation task and a baseline task. In the activation scans, the volunteers were presented with an English word every 5 s describing a common category of objects or concepts. After hearing a word, the volunteers were required to find an element belonging to the category just heard and name the element aloud (e.g., hear "flower," say "rose"; hear "religion," say "Buddhism"). The volunteers were instructed to say "pass" if they were unable to find a matching element. In the baseline tasks, English words were presented at the same rate as in the activation tasks. After hearing a word, the volunteers were required to repeat the word aloud. In all tasks, stimuli were presented binaurally through insert earphones (EarTone; Aearo Co., Indianapolis, IN) at an intensity of 75 dB (sound pressure level). The stimuli were matched, across scans, on a range of psycholinguistic parameters (e.g., length, syllable number, frequency, and part of speech).

Data Acquisition. The volunteers lay on the scanner bed with their eyes closed in a quiet darkened room. Each individual underwent scanning a total of 12 times: 3 activation/baseline and 3 baseline/activation scans using a switched protocol and 3 activation/baseline and 3 baseline/activation scans using a cold-bolus, switched protocol. The protocol and scan order used across individuals were counterbalanced to avoid random bias. All the scans were 3 min long. In each scan, a 3-s intravenous bolus injection of 15 mCi $H_2{}^{15}O$ was used. The volunteers rehearsed the activation and baseline tasks a few minutes before starting the scanning sessions using word lists similar but not identical to those used in the scans and were instructed to switch task execution (from activation to baseline or vice versa) at the presentation of an easily identifiable tone. The categories used while scanning were novel to the volunteers to minimize practice effects (*23,24*). The presentation of stimuli began once the bolus was injected. Data acquisition commenced 14 s later to account for the delay between tracer injection and arrival in the brain. Task switching occurred approximately 45 s after data acquisition began (~60 s after injection). After task switching, data acquisition continued for 135 s. In each scan using the combined protocol, a cold bolus was generated by isolating the vasculature of the lower limbs a few seconds before the injection of tracer using double cuffs applied to each upper thigh. To ensure total arterial and venous circulation block, the cuffs were inflated to a pressure level similar to that during surgical procedures using regional anesthesia (i.e., 400–500 mm Hg). In addition, the cessation of arterial circulation was verified by the loss of pulsation in the dorsal pedal artery on palpation. The cuffs

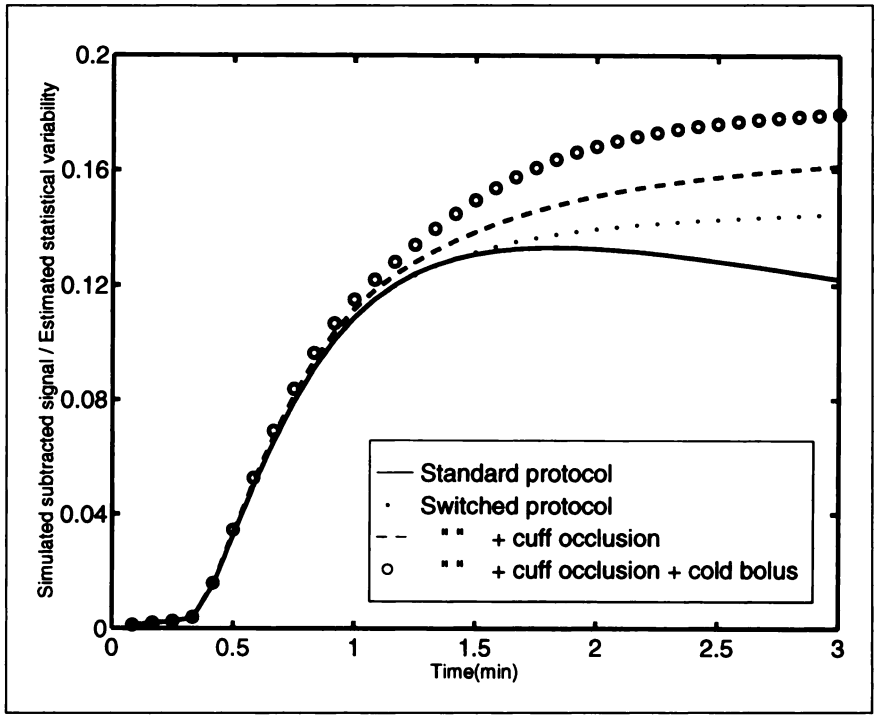

FIGURE 3. Relative magnitude of simulated subtracted signals with respect to their statistical uncertainty.

remained inflated until the subjects switched tasks and were rapidly deflated (~1 s) as soon as the first stimulus after task switching was presented. In addition to undergoing PET, all individuals underwent MRI to facilitate the identification of the anatomic structures associated with the PET images (*25*). The MR images were obtained using a 1.5-T Gyroscan (Philips Medical Systems, Best, The Netherlands) and consisted of 160 contiguous slices of 1-mm thickness and 1-mm^2 pixel size.

Image Analysis. Individual 3-dimensional scans were reconstructed and Hanning filtered (cutoff frequency, 0.3; image space resolution, 8 mm). Each dataset was corrected for isotope decay and scattered and random events. After reconstruction, the images were transformed into a stereotactic coordinate system (*26,27*) and normalized by mean whole-brain activity. The images were then grouped into 3 sets: switched protocol images; cold-bolus, switched protocol images; and an overall set containing all the acquired images. For each set, a *t* statistic image was generated for the mean change in normalized activity between baseline and activation scans using an SD pooled across all image voxels (*28*). The activation foci associated with the generation of elements from a category were identified in the dataset containing all the acquired images because this group was the largest sample. Corresponding activation foci were then identified in the other 2 groups and compared in terms of magnitude, statistical significance, and S/N. The statistical significance of the activation foci was determined using a previously described method based on gaussian random field theory (*28*). A focus was deemed statistically significant if the probability of its being false-positive was less than 5%. The anatomic location of activation foci was determined from the averaged-across-subjects coregistered MR volumes.

Characteristics of Expected Activation Foci. The cognitive tasks used in this study were a series of lexical search and retrieval operations. These operations have been studied extensively in our laboratories using healthy volunteers performing different cognitive tasks (*12,17,18*). Findings from those studies suggest that a distinct group of brain regions is activated when individuals execute these types of operations. The main activated brain regions are the left inferior frontal cortex, the left and right insular–opercular cortices, the right cerebellar cortex, the left inferotemporal cortex, and the left posterior parietal cortex. Among these regions, the most consistently activated area is that delimited by the left inferior frontal cortex and the left insular–opercular cortex, suggesting that this area may be directly involved in lexical search and retrieval operations (*17,18,23,29,30*). The right insular–opercular foci have been observed in only a fraction of the individuals studied, suggesting that this region may not be indispensable to performing this type of operation or that its involvement depends on the strategies of each individual when executing the tasks (*18*). The left inferotemporal cortex is believed to be involved in the processing of words (*17,18,23*). The roles of the left posterior parietal and right cerebellar cortices are not fully understood; nevertheless, similar foci have been detected in individuals performing a large range of lexical search operations (*17*).

Blood Circulation Occlusion and Blood Pressure Changes. The hemodynamic effects of cuff inflation on arterial blood pressure were measured at the brachial artery using sphygmomanometry and Korotkoff's sounds in 2 healthy volunteer groups containing 4 and 3 individuals. In the first group, measurements were obtained manually a few seconds before and 60 s after cuff inflation. In the second group, periodic measurements were obtained with an automatic blood-pressure meter (mean sampling rate, 25 s) before, during, and after cuff inflation over periods similar to those used to acquire the PET scans.

RESULTS

Simulation Studies

Results from the simulations suggest that the combined cold-bolus, switched protocol will enhance the signal from averaged subtracted images compared with equivalent signals obtained with standard or switched protocols. The simulations, which included the reduction in blood volume introduced by lower limb occlusion, showed a 14% increase in the integrated subtracted signal compared with the equivalent signal from the simulated switched protocol (Figs. 1 [input function B] and 2C [the integrated subtracted signal depicts the difference between the areas delimited by the activation and baseline simulated time–activity curves]). When the simulations also included a time-dependent mixing of the cold bolus, the integrated subtracted signal was 27% greater than the equivalent signal from the switched protocol (Figs. 1 [input function C] and 2D). The overall count variability (noise) in the averaged subtracted images for the protocols simulated was expected to remain fairly constant because the main factor affecting the overall image noise was the scan length (i.e., total collected counts), which was the same in all the simulated protocols.

Subtracted images acquired using the switched protocol yield a higher S/N than did matching standard-protocol images because the difference in activity concentration between activation and baseline states is maintained longer (Figs. 2A and B), allowing longer scanning times (*11,12*). The longer scanning times increase the S/N of the subtracted images through the reduction of image noise. The signal in switched-protocol images is maintained longer because the washout of tracer from activated regions is reduced during activation/baseline scans and washout from the activated regions is increased during baseline/activation scans. Cold-bolus, switched protocols extend this concept by manipulating the input function to enhance the subtracted signal while yielding noise levels similar to those obtained with switched protocols. This effect is accomplished by increasing the concentration of tracer delivered during the uptake phase and decreasing blood tracer concentration during the washout phase of the acquisition period. Because use of the cold bolus enhances the dissimilarity between 2 different flow states, the simulations also indicate that negative subtracted signals, resulting from either a flow increase in the baseline scans or a flow decrease in the activation scans, will increase in magnitude. Figure 3 shows the relative magnitude of the simulated accumulated counts (activation/baseline) with respect to their estimated statistical uncertainty. For the scans simulated here, the improvement yielded by the combined protocol is more than twice that obtained with the switched protocol.

PET Experiments

Figure 4 shows mean normalized whole-brain radioactivity for actual PET scans using the switched and combined

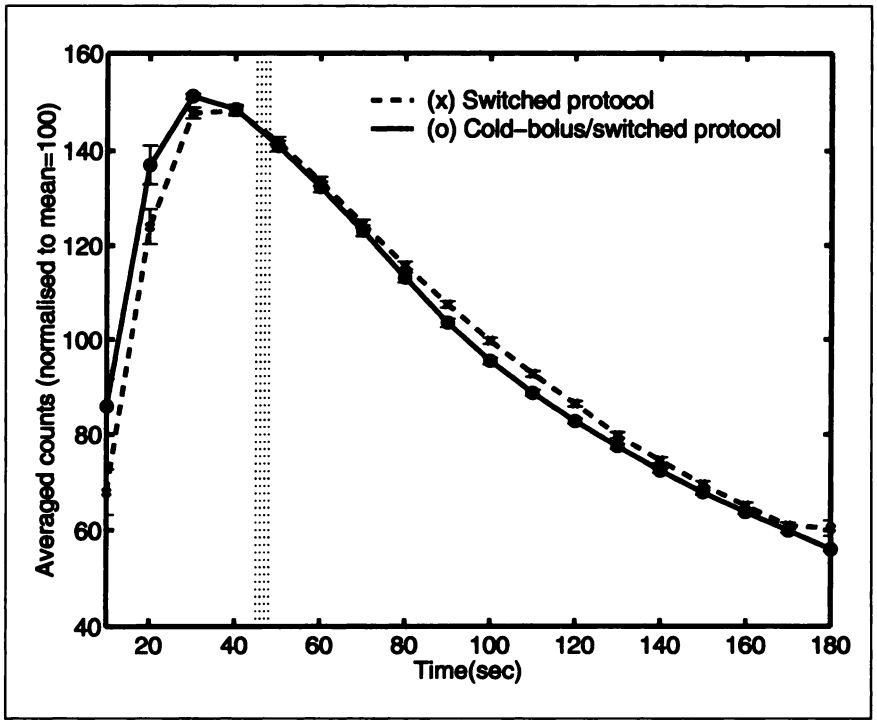

FIGURE 4. Effect of lower limb occlusion and cold-bolus release on observed non–decay-corrected whole-brain counts. At beginning of scanning, occlusion of blood circulation to lower limbs results in increase in counts. After cuffs are deflated, released cold bolus causes time-varying reduction in whole-brain counts.

protocols. The dotted vertical line in the figure indicates the time region where task switching and cuff deflation occurred. Compared with the switched protocol, the combined protocol yielded an increase in normalized activity while the cuffs remained inflated (uptake phase). This increase was probably caused by the reduction in the blood volume available for tracer mixing. After cuff deflation (washout phase), there was a reduction in normalized activity that was likely caused by the release of the large tracer-free bolus of blood. As expected, the effect of the cold bolus on tracer concentration was not immediate because the cold bolus does not reach the brain instantaneously. The effect appeared approximately 30 s after cuff deflation (Fig. 4; time, 80 s) and remained for approximately 50 s. Late during scanning, the difference between the whole-brain counts from switched and cold-bolus protocol scans decreased, because after the cold bolus is uniformly mixed, the 2 protocols are equivalent.

Improved Detection of Activation Foci. Table 1 shows the location, magnitude, and significance level of the brain regions that experienced statistically significant increases in activity concentration in the group containing all the acquired images. No statistically significant decreases were observed. The foci were located in the right cerebellum, left and right insula–opercula, and left frontomedial cortex. For all the foci, the *t* statistic was greater with the cold-bolus, switched protocol than with the switched protocol alone. The average increase was 36%. Because the *t* statistic is proportional to the magnitude of the averaged subtracted signal (m values in table) and inversely proportional to the overall image noise (pooled SD values in table), the results

TABLE 1
Location, Signal Magnitude, and Significance Level of Activation Foci

	Average "all" scans (pooled SD, 8.54)				Switched-protocol scans (pooled SD, 8.27)					Combined protocol scans (pooled SD, 8.76)						
Region	x	y	z	*t*	x	y	z	*t*	m	x	y	z	*t*	m	%Δ*t*	%Δm
Right cerebellum	38	−78	−32	6.1	38	−80	−32	4.2	12.2	35	−73	−33	6.1	20.0	45.2	63.9
Left insula–opercula	−38	20	−5	4.8	−43	22	−3	3.4	9.2	−36	20	−5	4.5	13.0	32.4	41.3
Right insula–opercula	31	20	−3	4.8	43	20	0	2.8	7.6	31	20	−3	4.6	13.4	64.3	76.3
Left frontomedial cortex	−1	13	59	6.2	−5	8	69	5.0	13.9	0	13	60	5.2	15.2	4.0	9.4

x, y, and z = location in Talaraich space; *t* = focus *t* statistic; m = focus signal magnitude; %Δ*t* and %Δm = relative increases obtained with combined protocol; pooled SD = mean voxel SD in averaged subtracted image.

Data are for activation foci believed to be associated with category generation task as indicated by statistical analysis of images in across-protocols set (Average "all" column). Values for equivalent foci detected in switched or cold-bolus, switched-protocol image sets are shown for comparison even if they did not reach statistical significance (Switched-protocol and Combined protocol columns, respectively).

shown in the table indicate that the increases in the t statistic were caused by increases in the signals from the subtracted images (%Δm shows signal changes across protocols) and not by changes in the overall image noise, which remained essentially constant. These observations agree with the simulations, which predicted an increase in the activation signals from the subtracted images (Figs. 2C and D). The image noise was not expected to change significantly because the acquisition time for the 2 protocols tested was the same. The variations in the degree of improvement to the t statistic observed among the detected foci may be caused by random noise and by differences in the time that brain regions were activated within scans with respect to cold-bolus dispersion patterns.

Category Generation as Lexical Search and Retrieval Operation. The foci activated when executing the category generation task closely match those in previous experiments monitoring lexical search and retrieval operations that used different cognitive tasks and standards as well as switched activation protocols (*12,17*). All statistically significant foci detected here had been observed previously. Foci were also detected in the left inferotemporal cortex ($x = -59$, $y = -52$, $z = -9$, $t = 3.26$) and left posterior parietal cortex ($x = -27$, $y = -68$, $z = 48$, $t = 3.61$), but the number did not reach statistical significance. These foci had been previously identified to be involved in lexical search and retrieval operations; however, the peaks found in the previous experiments were weak and were considered significant only when evidence from other psychologic experiments was included in the data analysis (*17,18*). The area delimited anteriorly by the left inferior frontal cortex and posteriorly by the insular–opercular cortex has been associated with search-and-retrieval tasks (*17,18,29*). A focus anterior to the left insular–opercular focus shown in the table was detected, but this focus, although relatively strong, did not reach our stringent level of statistical significance ($x = -50$, $y = 30$, $z = -2$, $t = 4.29$). Although a significant focus was expected in this area, evidence from single-subject experiments (*18*) suggests that the location of the left inferior frontal focus can be anywhere between the left inferior frontal cortex and the opercular cortex (*17,18*); the small number of individuals in this study may therefore explain why this commonly seen focus reached only a weak level of statistical significance.

Implementation of Cold-Bolus, Switched Protocol. The cold-bolus, switched protocol was simple to implement and well tolerated by all volunteers. The optimal time for cuff deflation was not investigated. However, evidence from switched-protocol experiments (*11*) suggests that the S/N gains yielded by the combined protocol are maximized if task switching—and therefore cuff deflation—takes place 20–30 s after brain counting rates peak. Further improvements in the S/N of activation images may be obtained if task switching and cuff-release times are adjusted to account for the blood circulation characteristics of each individual. However, this improvement would be at the expense of a more complex and unwieldy experimental protocol.

The apparatus required to create the cold bolus is portable and readily available, being commonly used for intravenous regional anesthesia. Cuff inflation may cause some discomfort (*31–33*), but this can be minimized by inflating the cuffs slowly. None of the volunteers thought that the discomfort interfered with performing the cognitive tasks. In healthy volunteers, no significant risk is associated with the use of cuffs for the periods required by the combined protocol (*31*), and cuff inflation and deflation did not produce significant changes in arterial blood pressure. However, caution is required when using this protocol on individuals likely to have cardiovascular disorders, such as the elderly, or on patients suffering from peripheral vascular disease, diabetes, or congestive cardiac failure. In these individuals, we recommend the use of alternative ways to increase the S/N of PET images (e.g., decrease image noise through dose fractionation strategies [*22*] and switched protocols [*11,12*]). Use of the cuffs did not generate additional statistically significant foci in the subtracted images, likely because the somatosensory effects of cuff inflation were constant across conditions.

CONCLUSION

We describe a data acquisition strategy for activation studies that combines the switched protocol with the release of a bolus of blood containing little or no activity at the time that task execution is switched. Simulation studies predict that the combined protocol will enhance the signal from activation foci, in comparison with the signal from equivalent images obtained using a standard or switched protocol. The protocol was tested using 48 3-dimensional PET scans from a group of 4 healthy volunteers performing a cognitive task. In this group, the combined protocol improved the significance of the activation signals by an average of 36%. The combined cold-bolus, switched protocol was simple to implement and well tolerated by all participants.

ACKNOWLEDGMENTS

The authors thank Pierre Ahad for help with preparing the auditory stimuli and the staff of the McConnell Brain Imaging Center for technical assistance during the acquisition and analysis of the PET data. This study was supported by the Medical Research Council of Canada (SP-30).

REFERENCES

1. Herscovitch P, Markham J, Raichle ME. Blood flow measured with intravenous $H_2{}^{15}O$: part 1. Theory and error analysis. *J Nucl Med.* 1983;24:782–789.
2. Raichle ME, Martin WR, Herscovitch P, Mintun MA, Markham J. Brain blood flow measured with intravenous $H_2{}^{15}O$: part 2. Implementation and validation. *J Nucl Med.* 1983;24:790–798.
3. Mazziota J, Huang SC, Phelps ME, Carson RE, MacDonald NS, Mahoney K. A noninvasive positron computed tomography technique using oxygen-15-labelled water for the evaluation of neurobehavioral task batteries. *J Cereb Blood Flow Metab.* 1985;5:70–78.
4. Roland PE. *Brain Activation.* New York, NY: Wiley-Liss; 1993.
5. Mazziotta JC, Phelps ME. Positron emission tomography studies of the brain. In: Phelps ME, Mazziotta JC, Schelbert HR, eds. *Positron Emission Tomography and*

Autoradiography: Principles and Applications for the Brain and Heart. New York, NY: Raven Press; 1986:493–579.
6. Fox PT, Mintun MA, Reiman EM, Raichle ME. Enhanced detection of focal brain responses using intersubject averaging and change-distribution analysis of subtracted PET images. *J Cereb Blood Flow Metab.* 1988;8:642–653.
7. Grafton S, Mazziotta J, Presty S, et al. Functional anatomy of human procedural learning determined with regional cerebral blood flow and PET. *J Neurosci.* 1992;12:2542–2548.
8. Kanno I, Iida H, Miura S, Murakami M. Optimal scan time of oxygen-15-labelled water injection method for measurements of cerebral blood flow. *J Nucl Med.* 1991;32:1931–1934.
9. Mintun MA, Raichle ME, Quarles RP. Length of PET data acquisition inversely affects ability to detect focal areas of brain activation [abstract]. *J Cereb Blood Flow Metab.* 1989;9(suppl 1):S349.
10. Volkow ND, Mullani N, Gould LK, Adler SS, Gatley SJ. Sensitivity of measurements of regional brain activation with oxygen-15-water and PET to time of stimulation and period of image reconstruction. *J Nucl Med.* 1991;32:58–61.
11. Cherry SR, Woods RP, Doshi NK, Banerjee PK, Mazziotta JC. Improved signal-to-noise in PET activation studies using switched paradigms. *J Nucl Med.* 1995;36:307–314.
12. Moreno-Cantú JJ, Reutens DC, Thompson CJ, et al. Signal-enhancing switched protocols to study higher-order cognitive tasks with PET. *J Nucl Med.* 1998;39: 350–356.
13. Albert SN. *Blood Volume and Extracellular Fluid Volume.* Springfield, IL: Charles C. Thomas; 1971:15–16.
14. Rowell LB. *Human Circulation: Regulation During Stress.* New York, NY: Oxford University Press; 1986:118.
15. Henry JP, Meehan JP. *The Circulation: An Integrative Physiologic Study.* Chicago, IL: Year Book Medical Publishers; 1971:20–21.
16. Kety SS. The theory and application of the exchange of inert gas at the lungs and tissues. *Pharmacol Rev.* 1951;3:1–41.
17. Klein D, Milner B, Zatorre RJ, Meyer E, Evans AC. The neural substrates underlying word generation: a bilingual functional-imaging study. *Proc Natl Acad Sci USA.* 1995;92:2899–2903.
18. Klein D, Zatorre RJ, Milner B, et al. CBF patterns during synonym generation: group vs. individual study. *Neuroimage.* 1996;3(suppl):S444.
19. Vafaee M, Murase K, Gjedde A, Meyer E. Dispersion correction for automatic sampling of O-15-labeled H_2O and red blood cells. In: Myers R, Cunningham V, Bailey D, Jones T, eds. *Quantification of Brain Function Using PET.* San Diego, CA: Academic Press; 1996:72–75.
20. Perlmutter JS, Powers WJ, Herscovitch P, et al. Regional asymmetries of cerebral blood flow, blood volume, and oxygen utilization and extraction in normal subjects. *J Cereb Blood Flow Metab.* 1987;7:64–67.
21. Frackowiak RSJ, Lenzi GL, Jones T, Heather JD. Quantitative measurement of regional cerebral blood flow and oxygen metabolism in man using ^{15}O and positron emission tomography: theory, procedure, and normal values. *J Comp Assist Tomogr.* 1980;4:727–736.
22. Moreno-Cantú JJ, Thompson CJ, Zatorre RJ. Evaluation of the ECAT EXACT HR+ 3D PET scanner in $H_2{}^{15}O$ brain activation studies: dose fractionation strategies for rCBF and signal enhancing protocols. *IEEE Trans Med Imaging.* 1998;17:979–985.
23. Raichle ME, Fiez VA, Videen TO, et al. Practice-related changes in human brain functional anatomy during nonmotor learning. *Cereb Cortex.* 1994;4:8–26.
24. Meyer E, Ferguson SS, Zatorre RJ, et al. Attention modulates somatosensory cerebral blood flow response to vibrotactile stimulation as measured by positron emission tomography. *Ann Neurol.* 1991;29:440–443.
25. Evans AC, Marret S, Torrescorzo J, Ku S, Collins L. MRI-PET correlation in three dimensions using a volume-of-interest (VOI) atlas. *J Cereb Blood Flow Metab.* 1991;11:A69–A78.
26. Evans AC, Marret S, Neelin P, et al. Anatomical mapping of functional activation in stereotactic coordinate space. *Neuroimage.* 1992;1:43–53.
27. Talairach J, Tournoux P. *Co-Planar Stereotaxic Atlas of the Human Brain.* New York, NY: Thieme Medical Publishers; 1988.
28. Worsley KJ, Evans AC, Marrett S, Neelin P. A three-dimensional statistical analysis for CBF activation studies in human brain. *J Cereb Blood Flow Metab.* 1992;12:900–918.
29. Petersen SE, Fox PT, Posner MI, Mintun M, Raichle ME. Positron emission tomographic studies of the cortical anatomy of single-word processing. *Nature.* 1988;331:585–589.
30. McCarthy G, Blamire AM, Rothman DL, Gruetter R, Shulman RG. Echo-planar magnetic resonance imaging studies of frontal cortex activation during word generation in humans. *Proc Natl Acad Sci USA.* 1993;90:4952–4956.
31. Murphy FL. Anaesthesia for orthopaedic surgery. In: Healy TE, Cohen PJ, eds. *Wylie and Churchill-Davidson's a Practice of Anaesthesia.* London, UK: Edward Arnold; 1995:1254–1255.
32. Hagenouw RRPM, Bridenbaugh PO, van Egmond J, Stuebing R. Tourniquet pain: a volunteer study. *Anaesthesiology.* 1986;65:1175–1180.
33. Sapega AA, Heppenstall RB, Chance B, Park YS, Sokolow D. Optimizing tourniquet application and release times in extremity surgery. *J Bone Joint Surg [Am].* 1985;67:303–314.